Plasma Chemistry and Plasma Processing, Vol. 5, No. 3, 1985

On the Use of Actinometric Emission Spectroscopy in SF_6–O_2 Radiofrequency Discharges: Theoretical and Experimental Analysis

R. d'Agostino,[1] F. Cramarossa,[1]
S. De Benedictis,[1] F. Fracassi,[1]
L. Láska,[2] and K. Mašek[2]

Received September 17, 1984; *revised January* 22, 1985

A comparison of the results obtained by solving the Boltzmann equation with the experimental results from optical emissions obtained in SF_6–O_2 radiofrequency discharges, when N_2, Ar, and He are also admitted as actinometers, has allowed us to explore the potentialities and limits of actinometry. The use of different actinometers also allowed us to monitor the evolution of the electron distribution functions as a function of the plasma parameters.

KEY WORDS: Actionometry; spectroscopy; etching; SF_6–O_2 discharge.

1. INTRODUCTION

Actinometric emission spectroscopy has been found to be one of the most powerful, nonintrusive, diagnostic techniques for understanding the role played by stable and unstable species present in a discharge. This technique has allowed the measurement of reactive atom and molecule concentrations by comparison of their optical emissions with those of one or more inert gases added to the discharge mixture and is becoming the most widely utilized diagnostic tool for several types of gas mixtures used for etching and deposition.[1-13] When more actinometers are admitted at one time, e.g., N_2, Ar, and He, their emissions can be utilized as probes of electrons at various threshold energies and give information on the evolution

[1] Centro di Studio per la Chimica dei Plasmi, C. N. R., Dipartimento di Chimica, Università di Bari, Via Amendola 173, 70126 Bari, Italy.
[2] Institute of Physics, Czechoslovakian Academy of Sciences, 180 40 Prague 8, Liben, Na Slovance 2, Czechoslovakia.

0272-4324/85/0900-0239$04.50/0

of the electron distribution function (EDF) as a function of a plasma parameter.[11-14]

The criteria for the utilization of the technique and its limits of validity to correct the emissions of different species have been discussed in Ref. 11 for CCl_4-Cl_2 discharges, while in Refs. 12-13 preliminary experimental and theoretical results for SF_6-O_2 discharges are compared and discussed.

In this paper we carry out a more comprehensive comparative analysis between the calculated EDF's and the species excitation rates and experimental emission trends of F and O atoms and of the actinometers N_2, Ar, and He in order to find the validity limits for proper utilization of the actinometric technique in SF_6-O_2 discharges.

The main interest for SF_6-O_2 radiofrequency discharges comes from their utilization in dry-etching[15] materials such as Si, SiO_2, and Si_3N_4 of great importance in silicon integrated circuits technology.

2. EXPERIMENTAL

The apparatus has been described in detail elsewhere.[2,3,15a] It consists of an alumina tube (1.8 cm i.d., 50 cm length) capacitively coupled to a 27-MHz generator by means of two external brass electrodes (5×5 cm) which conforms to the tube curvature. By utilizing a matching box the impedances were matched in order to reduce reflected power (≤5%). Power and peak-to-peak voltage (V_{pp}) were monitored continuously with a through-line wattmeter and a low-capacitance probe connected to an oscilloscope. The power level (50 W) was kept constant for all the experimental feed compositions explored (0-100% O_2-SF_6, pressure 1.00 torr, total gas flow rate 27 sccm). The values of V_{pp} are plotted in Fig. 1 as a function of the feed composition. It is convenient to consider the discharge as operating in two different regions as a function of the electrical conditions: region 1, at feed composition in the range 0-60% O_2, characterized by constant values of power and voltage across electrodes; region 2, at compositions in the range 60-100% O_2, with voltage increasing with oxygen percentage. Comparative analysis of the experimental results is restricted mainly to the conditions in which region 1 is operative, i.e., at constant voltage. An analysis of emission data is, in fact, difficult when voltage and current are varying simultaneously. The data of Fig. 1 are consistent with a decrease of energetic electrons at high oxygen content in the feed, as shown in Refs. 15a and 16.

The light emitted from the discharge was sampled axially through a sapphire window at the end of the tube and focused by means of a quartz lens onto the entrance slit of a 1-m Jarrel-Ash visible monochromator.

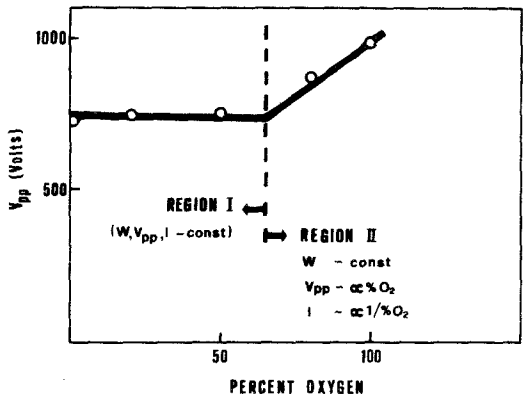

Fig. 1. Electrical characteristics (see text).

The spectroscopic analysis of SF_6–O_2 discharges has been discussed in Ref. 15a under similar experimental conditions. The spectral features followed for this work are: 703.7 nm atomic fluorine line, 777.5 nm atomic oxygen line, 750.3 nm argon line, 388.8 nm helium line, and 337.1 nm N_2 band of the second positive system.

3. THE BASIS OF ACTINOMETRY

It is worth clarifying some points of actinometry to avoid confusion, even though the principles of the technique have already been discussed in some detail in previous works.[2-9,11-14]

The technique consists of admitting into the feed small and constant amounts of "near" inert gases, such as N_2, Ar, and He, which do not modify the discharge characteristics. The method is based on the combination of measured intensities of emissions from actinometers and from discharge-emitting species. If we assume that excitation by direct electron impact prevails (stepwise excitation processes, excitation transfer between particles, and pair recombination of positive and negative ions can be omitted,[7] as well as cascading from higher excited states[1]), then the process for the generation and quenching of the optical emission is

$$e + X \rightarrow X^* + e \tag{1}$$

$$X^* \rightarrow X + h\nu \tag{2}$$

$$X^* + M \rightarrow X + M \tag{3}$$

where e, X, and M represent electrons, emitting species in the ground state, and third bodies, respectively.

At steady state the emission intensity of X^+, I_X, is correlated to the density of X, N_X, and of neutrals N by the expression

$$I_X \propto \frac{N_X \eta_X}{1 - NK_Q/A_{X^*}} \tag{4}$$

In Eq. (4) η_X represents the excitation efficiency of X by means of electrons with energy higher than the energy threshold ε_{th}; K_Q and A_{X^*} are collisional deactivation rate coefficient and transition probability for X^* spontaneous emission. Usually, the term NK_Q/A_{X^*} is assumed to be either less than 1 at low pressure ($P \lesssim 1$ torr) or constant at higher pressures,[2,3] and Eq. (4) can be simplified into

$$I_X \propto N_X \eta_X \tag{5}$$

The excitation efficiency can be expressed as follows:

$$\eta_X = N_e \sqrt{\frac{2e_0}{m}} \int_{\varepsilon_{th}}^{\infty} \sigma_{X^*}(\varepsilon)\, \varepsilon f(\varepsilon)\, d\varepsilon = N_e Z_X \tag{6}$$

Here, e_0 and m denote electron charge and mass, $\sigma_{X^*}(\varepsilon)$ is the cross section of excitation, $f(\varepsilon)$ is the electron distribution function, EDF, and Z_X is the excitation rate coefficient. Equations (1)-(6) are valid both for emitting species and actinometers. From these, we easily obtain

$$\frac{I_X}{I_{act}} \propto \frac{N_X}{N_{act}} \frac{\eta_X}{\eta_{act}} = \frac{N_X}{N_{act}} \frac{Z_X}{Z_{act}} \tag{7}$$

If the ratio of excitation efficiencies or rate coefficient of the emitting species and of the actinometer does not depend on the discharge parameter subject to variation, one gets the simple actinometric equation

$$\frac{I_X}{I_{act}} \propto \frac{N_X}{N_{act}} \tag{8}$$

which allows measurement of the concentration trends of X from the variation of I_X/I_{act} when N_{act} is known or kept constant.

Equation (8) deserves some comment because its validity depends on the constancy of the term Z_X/Z_{act} which, however, can vary as a consequence of:

(a) differences in the shapes of $\sigma(\varepsilon)$;
(b) differences in the values of ε_{th} of species and actinometer.

While the differences in the cross-section shapes have not been found to introduce large deviations from Eq. (8),[9,12] point (b) is more crucial and must be duly taken into consideration to avoid errors in the use of Eq. (8). The general behavior which should be followed for the utilization of Eq. (8) is either to correct only the emissions of those species which closely match the actinometer in energy or to make use of several actinometers

with different thresholds in order to extend the range of ε_{th} of the emitting species which can be corrected with this technique. In this last case it is possible to get information also on the evolution of the EDF at various energies. In Ref. 11, where use has been made of N_2, Ar, and He as actinometers for CCl_4–Cl_2 discharges, it has been shown that the ratios of the various excitation rate coefficient, Z_i/Z_j, including those of the actinometers, become independent of electron energy at the higher energies. When these conditions are attained, use of Eq. (8) can be extrapolated even for species with threshold energy much lower than that of the actinometers.

In this paper we compare the experimental results obtained with N_2, Ar, and He actinometers added to SF_6+O_2 mixtures with the calculations of the effect of the feed composition (SF_6/O_2) and of the amount of added actinometer on the variations of EDF and on the various Z_i/Z_j ratios.

The results obtained confirm the validity of the technique for these mixtures also and allow us to find its limits.

4. CALCULATION ON EDF AND EXCITATION RATE COEFFICIENTS

EDF's are obtained by solving the Boltzmann equation. The usual technique, described in Ref. 17, was applied for the numerical treatment of the Boltzmann equations, which is parametric in E/N and in the mixture composition. The mixtures explored are SF_6+O_2, SF_6+O_2+Ar, He, N_2, and SF_6+Ar, He. In the calculations we have used cross sections for electron collisions with O_2, SF_6, and N_2 molecules and He atoms from Refs. 17–19. Modified values from Ref. 20 were used for argon atoms: these were fitted to the measured electron mobility and the Townsend ionization coefficient.

In Fig. 2 we report the EDF in pure SF_6 and pure O_2 (Fig. 2A), in $SF_6+10\%$ Ar, He, and N_2 (Fig. 2B), and in ($SF_6+20\%$ O_2)$+10\%$ Ar, He, N_2 (Fig. 2C) for $E/N=10^{-15}$ V cm^2. It is shown in the figure that the number of low-energy electrons in the distribution, i.e., those below the EDF crossing, increases with oxygen addition. This effect is confirmed by the EDF calculated for the SF_6–O_2 mixtures and is evidenced by the decrease of mean electron energy, $\bar{\varepsilon}$. It should, however, be stressed that at higher E/N values the opposite behavior occurs.[16] Crossing of calculated EDF occurs approximately at 6 eV.

Addition of 10% N_2, Ar, and He to the mixtures modifies to some extent the EDF. It is shown in the figure that N_2 introduces the greatest modification by increasing the low-energy electrons; this is due to the large energy losses for vibrational excitation. On the contrary, He and Ar increase high-energy electrons ($\gtrsim$6 eV). This effect is more marked with helium, while argon introduces only negligible effects.

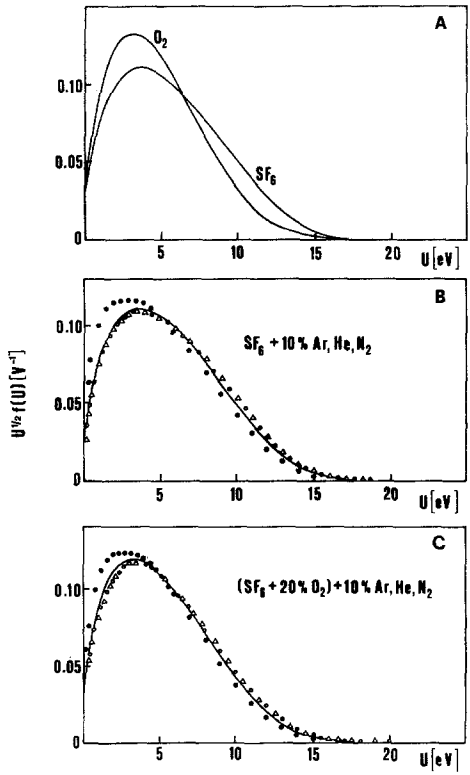

Fig. 2. Calculated electron distribution functions for $E/N = 1 \times 10^{-15}$ V cm^2 in : (A) pure SF_6 and pure O_2; (B) SF_6+10% Ar, He, N_2; (C) (SF_6+20% O_2)+10% Ar, He, N_2. Symbols: (●) N_2; (△) Ar; (○) He. Solid lines in (B) and (C) refer to pure SF_6 and SF_6+20% O_2, respectively.

The excitation rate coefficients Z_i for the excitations of nine states of monitored particles have been independently calculated for three ternary mixtures, (SF_6+20% O_2)+actinometer, as a function of the amount of added actinometer by making use of the calculated EDF and cross sections plotted in Fig. 3 and tabulated in Table I.

In Fig. 4 Z_i's are plotted vs. actinometer percentage in 20% O_2-SF_6 mixtures. The figure shows that:

1. The excitations of the various states are only slightly modified by argon admission, while admission of He increases generally all the excitations ($\varepsilon_{th} > 6$ eV) and admission of N_2 decreases the excitation rates of the various states.
2. The excitation rates of the $3p^2p$ and $3p^1p$ states of He are the most sensitive to actinometer additions.

Table I. Emission Wavelengths, λ, Thresholds, ε_{th}, and References for Excitation Cross-Sections, Q, for Various Transitions. In the Absence of Cross-Section Data these were Replaced by Argon-Like Curves. Z_i's are the Order of Magnitude Values of the Excitation Rate Coefficients

Number	Gas	ε_{th} (eV)	Q	Z_i	λ (nm)	Transition
1	O	10.73	Ar(5)	E-11	777.5	$3p^5P$-$3s^5S$
2	O	10.73	Ar(4)	E-10	777.5	$3p^5P$-$3s^5S$
3	N_2	11.00	Ref. 21	E-11	337.1	(0, 0) SPS
4	Ar	11.83	Ref. 24	E-11	—	$4s'(1/2)$
5	Ar	13.47	Ref. 23	E-11	750.3	$4p'(1/2)$-$4s'(1/2)$
6	F	14.74	Ar(5)	E-12	703.7	$3p^2P$-$3s^2P$
7	F	14.74	Ar(4)	E-12	703.7	$3p^2P$-$3s^2P$
8	He	23.00	Ref. 17, 22	E-16	388.9	$3p^3P$-$2s^3S$
9	He	23.06	Ref. 21	E-17	501.6	$3p^1P$-$2s^1S$

3. The excitation rates actually depend more on threshold energy than on cross-section shape, as suggested in Section 3.

Point 3 can be deduced by a comparative inspection of Figs. 3 and 4: the cross sections for helium states differ in shape and have the same ε_{th}. In fact, Z_i for both states vary with the same lows in the various cases considered.

In Fig. 5 we plot the ratios of the excitation rates, Z_i/Z_j, for O and F atom states (state i) and for the actinometers (j) as a function of the

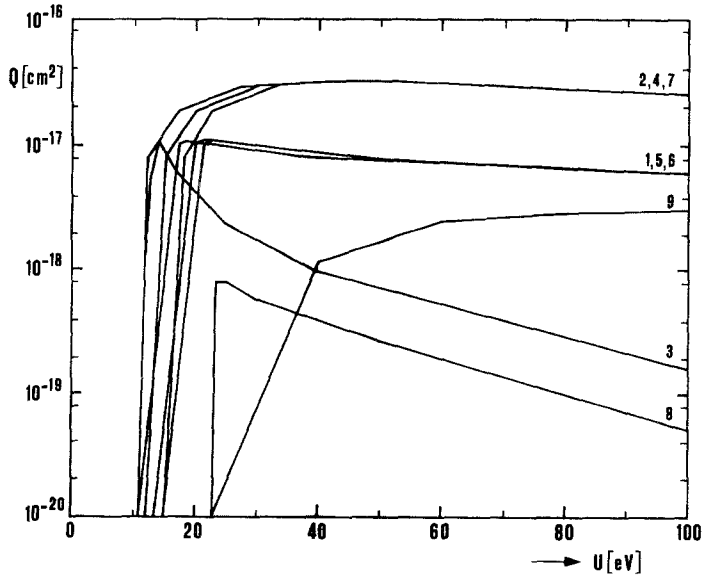

Fig. 3. Cross sections of Table I.

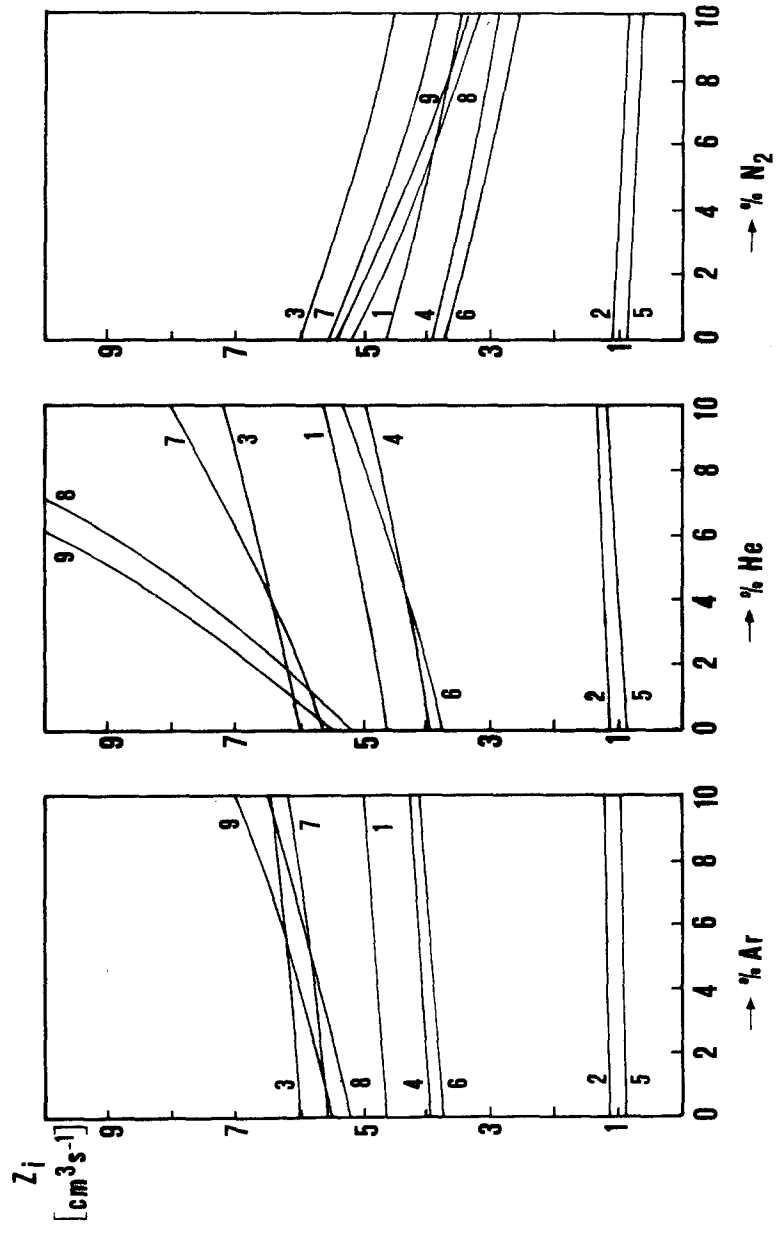

Fig. 4. Excitation rate coefficients in the mixtures with 20% oxygen. Numbering of the curves is according to Table I. Each curve has a different order of magnitude on the vertical scale, according to Table I.

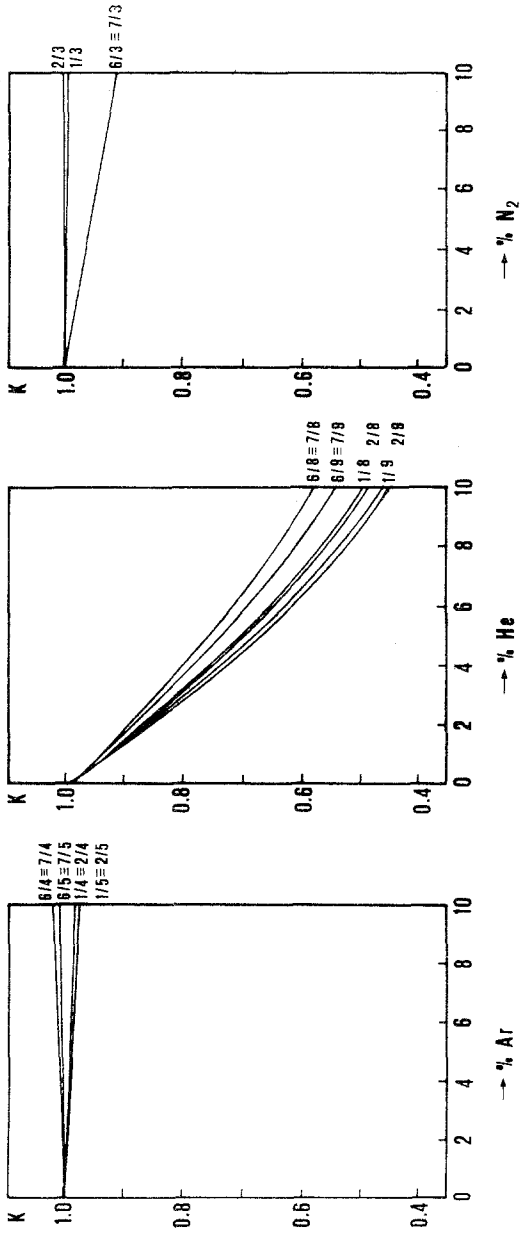

Fig. 5. Ratios of the different excitation rates from Fig. 4. Numbering of the symbolic fractions according to Table I.

actinometer addition to a SF_6 feed. If the term Z_i/Z_j is constant, the equation of actinometry, (8), can be utilized to correct emission from state i with actinometer j. Among the gases considered here and for the given compositions of the etching mixtures, argon is the best actinometer up to ~10% addition. Use of N_2 introduces only a small distortion (up to 8%) for F atoms when the N_2 is admitted in large amounts, while the distortion is negligible either for O or F atoms below 3% N_2. Helium causes large distortions with its admission (around 10% when 1% He is admitted). Distortions of Z_i/Z_j caused by helium admission can be ascribed to the large differences between the ε_{th}'s of F or O atoms and helium. In Ref. 11 it has been shown that distortion decreases when E/N and $\bar{\varepsilon}$ are increased.

5. EXPERIMENTAL RESULTS

The experimental results are collected in Fig. 6, where relative emissions of N_2, Ar, He, F, and O, as well as I_{Ar}/I_{N_2} and I_{He}/I_{Ar}, are plotted as a function of oxygen percent in SF_6-O_2 mixtures when a constant flow of

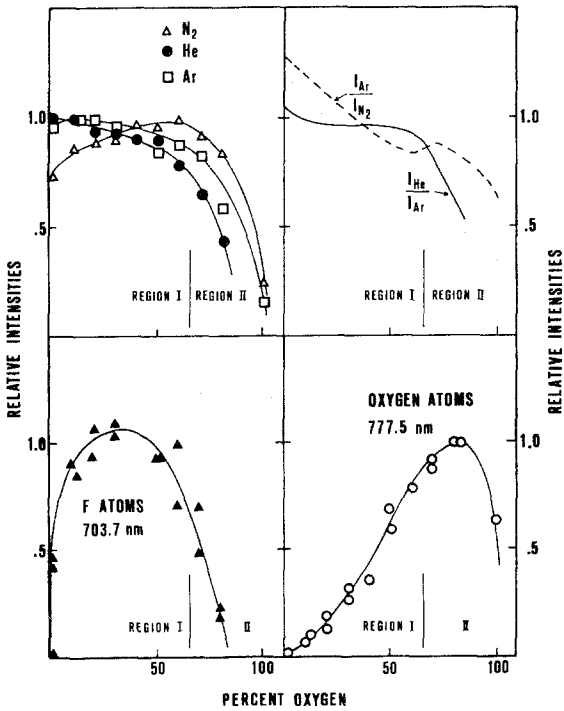

Fig. 6. Emissions of actinometers, and their ratios, of F atoms and oxygen atoms as a function of the oxygen percentage in the feed.

actinometer (~2%) was added to the feed. It is evident that in region II there is, generally, a steeper decrease of emissions, as pointed out in Section 2; however, our analysis will be limited to region I where the electrical parameters are kept constant.

A feature of actinometer emission is that N_2 intensity increases when the percent oxygen is increased, while Ar and He decrease (helium more markedly). This means that addition of oxygen enriches the EDF with electrons of energies ~11 eV (N_2) at the expense of high-energy electrons, i.e., ~14 eV (Ar) and ~23 eV (He). The trends of the ratios of actinometer emissions give the same indications; in fact I_{Ar}/I_{N_2} decrease markedly while I_{He}/I_{Ar} decrease at a low extent.

The behavior of actinometer emissions is in good qualitative agreement with the calculated evolution of EDF when oxygen is added to a SF_6 feed, as shown in Fig. 2. It should, however, be stressed that the experimental results are consistent with EDF crossing between ~11 eV (N_2) and ~14 eV (Ar), while calculations lead to crossing at lower energy. The discrepancies may be due to the nonuniformity of the electric field, which would lead to an erroneous estimation of experimental values of E/N, and/or excessive approximations in some evaluated cross sections, as discussed in Section 4.

The F and O atom emissions at 703.7 and 777.5 nm, respectively, are also plotted in Fig. 5. The experimental trends are consistent with previous results obtained under similar conditions[3,25] and mirror the trends of both electrons responsible for the excitations and electrons which induce dissociations in SF_6–O_2 mixtures. This duality can explain the unexpected behavior of oxygen atom emission in region II.

In Fig. 7 we report I_F/I_{Ar}, I_F/I_{N_2}, and I_O/I_{N_2} vs. percent oxygen. A theoretical analysis of Section 4 led to the conclusion that Ar and N_2 are the best actinometers for use with F and O atoms, respectively, and that

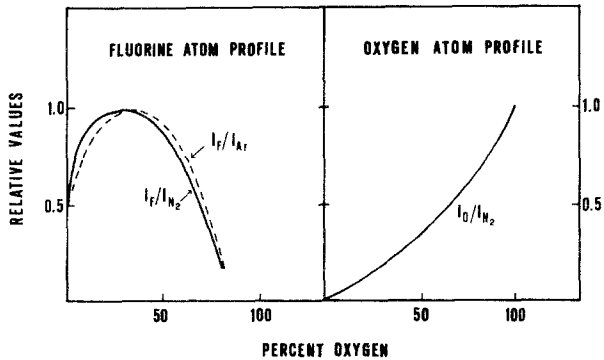

Fig. 7. I_F/I_{N_2}, I_F/I_{Ar}, and I_O/I_{Ar} as a function of the oxygen percentage in the feed.

N_2 introduces a low distortion at low percentages. This effect is also shown in the figure: in fact, the curve I_F/I_{Ar}, which should represent the concentration trend of F atoms according to Eq. (8), slightly differs from the curve I_F/I_{N_2}, particularly at low oxygen content in the feed. It is worth mentioning that the values of I_F/I_{N_2} and I_F/I_{Ar} at 20% O_2 can be made to coincide by simply multiplying I_F/I_{N_2} by the theoretical distortion ratio K_{Ar}/K_{N_2} as obtained by the curves in Fig. 5. It can be seen from the figure that actinometric correction of oxygen emission leads to a predictable rising trend with percent oxygen.

The bell-shaped F atom concentration trend is a known phenomenon both in SF_6-O_2 and in CF_4-O_2 etching mixtures. In Ref. 16 it is shown that, in correspondence with a maximum F atom concentration (~30%), there is a crossing of: (a) the rate of direct production of F atoms (i.e., $e+SF_X \rightarrow SF_{X-1}+F^-$ and $e+SF_X \rightarrow SF_{X-1}+F+e$), which decreases with % O_2, and (b) the rate of direct production of O atoms, which increases with % O_2. Oxygen atoms produced in the discharge react with SF_X radicals leading to SOF_2, SOF_4, and SO_2F_2 and freeing F atoms, through an overall bimolecular process.[25,26]

The effect of the introduction of the actinometers in a SF_6-O_2 feed is analyzed in Fig. 8 with respect to the emissions of F, O, and the actinometers. In this figure emissions are plotted as a function of actinometer addition to a 20% O_2-SF_6 feed. It can be seen that the 777.5 nm emission of oxygen remains constant, at least up to 10% addition of different actinometers, even though one should expect a small decrease due to the dilution effect. The 703.7 nm emission of fluorine atoms starts to decrease in all cases if the amount of actinometer gases reaches about 3–5% of total pressure. This value, hence, affects the experimental limiting amounts of actinometer gas admission in SF_6-O_2 discharges. Higher admissions must be avoided because they introduce modifications of the plasma media.

It should be noted from the figure that the decrease of F emissions cannot be explained by the small dilution effect.

Finally, the emissions of the actinometers are nearly linear with percent addition of the respective actinometer. Linearity of actinometer trends implies that its admission does not greatly change the electron densities at energies higher than about 11 eV (see Fig. 2). As for the production mechanisms of oxygen and fluorine atoms, the dissociation of oxygen (dissociative attachment) starts at 4.2 eV,[27] while the threshold energy for the same process for SF_6 is only a little above zero.[25] For this reason one should expect an increase of F atom production with nitrogen addition, because it enriches the EDF with low-energy electrons. The observed opposite trend of fluorine atoms with nitrogen should probably imply a selective chemical

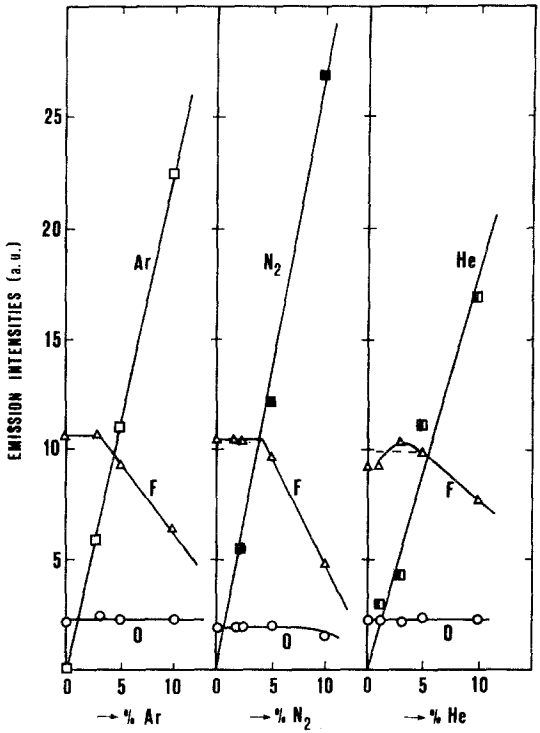

Fig. 8. Measured intensities of the monitored excited particles in 20% O_2–SF_6 mixtures as a function of the actinometer percentage admixtures.

interaction of nitrogen with other particles in the plasma, when its admission is higher than 3–5%.

6. CONCLUSIONS

Admission of different actinometer gases in dry-etching plasmas is of great utility because the technique is simple, fast, and nonintrusive and allows some inportant discharge parameters to be controlled. The theoretical and experimental analysis carried out in SF_6–O_2 radiofrequency discharges has allowed us to explore the potentialities and limits of the technique. The main features are:

1. Using different actinometers, N_2, Ar, and He, the evolution of the EDF with plasma parameters can be monitored because actinometers act as probes of electrons at various ε_{th}'s.

2. The maximum allowable admission of actinometers is in the range 3–5%. Higher concentrations lead to changes of discharge media.
3. Argon can be utilized as a tracing element for F and O atoms without introducing distortions, and N_2 can be used for O atoms while for F atoms it can be utilized only at low concentrations. Helium cannot be utilized for fluorine and oxygen in SF_6–O_2 discharges at low mean energies.[11]

ACKNOWLEDGMENT

We thank Mr. V. Colaprico for technical assistance.

REFERENCES

1. J. W. Coburn and M. Chen, *J. Appl. Phys.* **51**, 3134 (1980).
2. R. d'Agostino, F. Cramarossa, S. De Benedictis, and G. Ferraro, *J. Appl. Phys.* **52**,1259 (1981).
3. R. d'Agostino, V. Colaprico, and F. Cramaross, *Plasma Chem. Plasma Process.* **1**, 365 (1981).
4. R. d'Agostino, F. Cramarossa, and S. De Benedictis, *Plasma Chem. Plasma Process.* **2**, 213 (1982).
5. R. d'Agostino, F. Cramaross, V. Colaprico, and R. d'Ettole, *J. Appl. Phys.* **54**, 1284 (1983).
6. S. De Benedictis, M. Capitelli, F. Cramarossa, R. d'Agostino, and C. Gorse, *Opt. Commun.* **47**, 107 (1983).
7. S. K. Vinogradov, L. S. Polak, D. I. Slovetsky, and T. V. Fedoseeva, *Proc. XVth Intern. Conf. Phenom. Ionized Gases*, Minsk, 1981, p. 325.
8. V. M. Dolgopov, L. E. Pereversev, D. I. Slovetsky, and E. V. Shelykhanov, *Khim. Vys. Energ.* **16**, 350 (1982).
9. H. J. Tiller, D. Berg, and R. Mohr, *Plasma Chem. Plasma Process.* **1**, 247 (1981).
10. R. A. Gottscho, G. P. Davis, and R. H. Burton, *Plasma Chem. Plasma Process.* **3**, 183 (1983).
11. R. d'Agostino, F. Cramarossa, S. De Benedictis, and F. Fracassi, *Plasma Chem. Plasma Process.* **4**, 163 (1984).
12. L. Láska, K. Mašek, and R. d'Agostino, 5th Symp. Element. Process. Chem. React. in Low Temp. Plasma, Bauska Stiavnica, 1984, *Acta Phys. Slovaca* **35**, 199 (1984).
13. R. d'Agostino, V. Colaprico, F. Cramarossa, L. Láska, and K. Mašek, *Proc. 7th Eur. Sect. Conf. At. Mol. Phys. Ionized Gases*, (7th ESCAMPIG), Bari, 1984. p. 107.
14. S. De Benedictis, R. d'Agostino, and F. Cramarossa, *J. Appl. Phys.* **56**, 3198 (1984; *J. Phys. D* **18**, 413 (1985).
15. (a) R. d'Agostino and D. L. Flamm, *J. Appl. Phys.* **52**, 162 (1981); (b) R. d'Agostino, V. Colaprico, and F. Cramarossa, *Plasma Chem. Plasma Process.* **1**, 365 (1981).
16. K. Mašek, L. Láska, V. Peřina, and J. Krasa, *Acta Phys. Slovaca* **33**, 145 (1983).
17. K. Mašek, B. Kraliková, and J. Skála, *Czech. J. Phys. B* **30**, 885 (1980).
18. L. E. Kline, D. K. Davies, C. L. Chen, and P. J. Chantry, *J. Appl. Phys.* **50**, 6789 (1979).
19. K. Mašek, *Czech. J. Phys. B* **34**, 655 (1984).
20. J. Fletcher and D. S. Burch, *J. Phys. D* **5**, 2037 (1972).
21. J. W. Glaagher and E. C. Beaty, JILA Information Center Rep. No. 13 (1973).
22. S. J. B. Corrigan and A. von Engel, *Proc. Phys. Soc. London A* **22**, 786 (1958).
23. I. P. Zapesotchny and P. V. Feltsan, *Opt. Spectrosc.* **20**, 21 (1965).

24. L. R. Petterson and J. E. Allen, *J. Chem. Phys.* **56**, 6068 (1972).
25. R. d'Agostino and D. L. Flamm, *J. Appl. Phys.* **52**, 162 (1981).
26. R. d'Agostino, V. Colaprico, and F. Cramarossa, *Proc. 14th National Congress of Inorganic Chemistry*, F13, 1981.
27. L. Láska, K. Mašek, and T. Růžička, *Czech. J. Phys. B* **29**, 498 (1983).